

$CeAu_2In_4$: A candidate of quasi-one-dimensional antiferromagnetic Kondo lattice

Meng Lyu(吕孟), Hengcan Zhao(赵恒灿), Jiahao Zhang(张佳浩), Zhen Wang(王振), Shuai Zhang(张帅), and Peijie Sun(孙培杰)

Citation: Chin. Phys. B, 2021, 30 (**8**): 087101. DOI: 10.1088/1674-1056/ac0a60
Journal homepage: http://cpb.iphy.ac.cn; http://iopscience.iop.org/cpb

What follows is a list of articles you may be interested in

Two ultra-stable novel allotropes of tellurium few-layers

Changlin Yan(严长林), Cong Wang(王聪), Linwei Zhou(周霖蔚), Pengjie Guo(郭朋杰), Kai Liu(刘凯), Zhong-Yi Lu(卢仲毅), Zhihai Cheng(程志海), Yang Chai(柴扬), Anlian Pan(潘安练), Wei Ji(季威)
Chin. Phys. B, 2020, 29 (**9**): 097103. DOI: 10.1088/1674-1056/aba606

Possible nodeless $s^{\pm}$-wave superconductivity in twisted bilayer graphene

Zhe Liu(刘哲), Yu Li(李宇), Yi-Feng Yang(杨义峰)
Chin. Phys. B, 2019, 28 (**7**): 077103. DOI: 10.1088/1674-1056/28/7/077103

Global phase diagram of a spin-orbit-coupled Kondo lattice model on the honeycomb lattice

Xin Li(李欣), Rong Yu(俞榕), Qimiao Si
Chin. Phys. B, 2019, 28 (**7**): 077102. DOI: 10.1088/1674-1056/28/7/077102

Heavy fermions in high magnetic fields

M Smidman, B Shen(沈斌), C Y Guo(郭春煜), L Jiao(焦琳), X Lu(路欣), H Q Yuan(袁辉球)
Chin. Phys. B, 2019, 28 (**1**): 017106. DOI: 10.1088/1674-1056/28/1/017106

Pressure effect in the Kondo semimetal $CeRu_4Sn_6$ with nontrivial topology

Jiahao Zhang(张佳浩), Shuai Zhang(张帅), Ziheng Chen(陈子珩), Meng Lv(吕孟), Hengcan Zhao(赵恒灿), Yi-feng Yang(杨义峰), Genfu Chen(陈根富), Peijie Sun(孙培杰)
Chin. Phys. B, 2018, 27 (**9**): 097103. DOI: 10.1088/1674-1056/27/9/097103

RAPID COMMUNICATION

$CeAu_2In_4$: A candidate of quasi-one-dimensional antiferromagnetic Kondo lattice*

Meng Lyu(吕孟)[1,2], Hengcan Zhao(赵恒灿)[1], Jiahao Zhang(张佳浩)[1,2], Zhen Wang(王振)[1,2], Shuai Zhang(张帅)[1,2], and Peijie Sun(孙培杰)[1,2,3,†]

[1] *Beijing National Laboratory for Condensed Matter Physics, Institute of Physics, Chinese Academy of Sciences, Beijing* 100190, *China*
[2] *University of Chinese Academy of Sciences, Beijing* 100049, *China*
[3] *Songshan Lake Materials Laboratory, Dongguan* 523808, *China*

(Received 28 April 2021; revised manuscript received 7 June 2021; accepted manuscript online 11 June 2021)

Needle-like single crystals of $CeAu_2In_4$ have been grown from In flux and characterized as a new candidate of quasi-one-dimensional Kondo lattice compound by crystallographic, magnetic, transport, and specific-heat measurements down to very low temperatures. We observe an antiferromagnetic transition at $T_N \approx 0.9$ K, a highly non-mean-field profile of the corresponding peak in specific heat, and a large Sommerfeld coefficient $\gamma = 369$ mJ·mol^{-1}·K^{-2}. The Kondo temperature T_K is estimated to be 1.1 K, being low and comparable to T_N. While Fermi liquid behavior is observed deep into the magnetically ordered phase, the Kadowaki–Woods ratio is much reduced relative to the expected value for Ce compounds with Kramers doublet ground state. Markedly, this feature shares striking similarities to that of the prototypical quasi-one-dimensional compounds $YbNi_4P_2$ and $CeRh_6Ge_4$ with tunable ferromagnetic quantum critical point. Given the shortest Ce–Ce distance along the needle direction, $CeAu_2In_4$ appears to be an interesting model system for exploring antiferromagnetic quantum critical behaviors in a quasi-one-dimensional Kondo lattice with enhanced quantum fluctuations.

Keywords: heavy fermion, quasi-one-dimensional, Kondo lattice, magnetic phase transition

PACS: 71.27.+a, 71.20.Eh, 72.15.–v **DOI:** 10.1088/1674-1056/ac0a60

1. Introduction

Dimensionality provides distinct opportunities to tune the spin fluctuations and the f-conduction band hybridization in Kondo-lattice compounds.[1] A good demonstration of such effect can be found in superlattice of $CeIn_3/LaIn_3$ where the antiferromagnetic (AFM) transition temperature (T_N) of bulk $CeIn_3$ is gradually suppressed and a non-Fermi liquid emerges when the superlattice period is reduced.[2] As has been frequently addressed in geometrically frustrated systems, low dimensional arrangement of quantum spins offers, as well, an effective way to enhance quantum spin fluctuations. As far as Kondo-lattice compounds are concerned, quantum fluctuations favored by low dimensionality will add an additional tenability to the interplay between the Kondo effect and the Ruderman–Kittel–Kasuya–Yosida (RKKY) interaction, paving a way for realizing emergent quantum phases beyond the Doniach phase diagram.[3] Thus far, quasi-two-dimensional (q2D) Kondo-lattice compounds such as $YbRh_2Si_2$[4] and $CeCoIn_5$[5] have been extensively investigated, unveiling a prototype of unconventional quantum critical point (QCP) with Kondo destruction or unconventional superconductivity. By contrast, quasi-one-dimensional (q1D) Kondo-lattice compounds remain largely unexplored. Among the few cases of q1D Kondo-lattice compounds, $YbNi_4P_{2-x}As_x$[6] and $CeRh_4Ge_6$[7] show a ferromagnetic (FM) QCP, a rare realization that has not been confirmed in q2D counterparts, when their ferromagnetic orders are suppressed by chemical and hydrostatic pressures, respectively. In q1D Kondo lattice $CeCo_2Ga_8$,[8] a non-Fermi liquid ground state, ascribed to the enhanced spin fluctuations, has been observed.

Aiming at further insight into the competing low-energy states in q1D Kondo lattices, in this work, we have synthesized and investigated the low-temperature physical properties of single crystalline $CeAu_2In_4$ and its nonmagnetic analogue $LaAu_2In_4$. While Salvador *et al.* have first reported the single crystal synthesis of RAu_2In_4 (R = La, Ce, Pr, and Nd) from In flux and solved their crystal structure as being orthorhombic with the space group *Pnma* (No. 62).[9] RAu_2In_4 with heavy rare earth, e.g., $YbAu_2In_4$, was reported to adopt a different structure, being monoclinic with the space group $P2_1/m$.[10] Magnetic properties of $CeAu_2In_4$ at $T > 2$ K have been reported briefly,[11] which are already intriguing. While Curie–Weiss behavior arising from magnetic Ce^{3+} ions is confirmed at high temperatures, this compound remains paramagnetic down to 2 K. A likely incipient magnetic ordering with

*Project supported by the National Natural Science Foundation of China (Grant Nos. 11774404 and 52088101), the National Key R&D Program of China (Grant No. 2017YF A0303100), and the Chinese Academy of Sciences through the Strategic Priority Research Program (Grant No. XDB33000000).

†Corresponding author. E-mail: pjsun@iphy.ac.cn

© 2021 Chinese Physical Society and IOP Publishing Ltd

strong spin fluctuations is indicated by the specific heat divided by temperature, C/T, which reveals a significant enhancement below $T = 4$ K. On the other hand, the hybridization between the f and conduction bands is weak because of the lack of apparent Kondo-effect feature in electrical resistivity, namely, the $-\ln T$ dependence of resistivity. Whether low dimensionality rather than the Kondo effect is highly relevant in determining the ground-state physics appears to be an intriguing problem of current interest.[12]

Through detailed measurements of electrical resistivity, dc and ac susceptibilities, and specific heat down to very low temperatures of approximately 0.1 K, an AFM transition at $T_N \approx 0.9$ K was confirmed for $CeAu_2In_4$. A large Sommerfeld coefficient of the specific heat, $\gamma = 369$ mJ·mol^{-1}·K^{-2}, was obtained in the magnetically ordered phase. Fermi-liquid behavior was observed below T_N in resistivity. However, the Kadowaki–Woods (KW) ratio, namely, the ratio of A (the coefficient of the quadratic term in resistivity) and γ^2, is much smaller than that expected for heavy-fermion compounds with a Kramers doublet ground state. The unusual KW ratio is similar to that observed in q1D Kondo lattice compounds $YbNi_4P_2$[13] and $CeRh_6Ge_4$.[7] Given the apparent signatures of strong quantum spin fluctuations in the vicinity of the AFM ordering, we propose this compound to be a new candidate of q1D Kondo lattice with suppressed antiferromagnetism, suited for further exploration of unconventional quantum critical phenomena.

2. Experimental details

Single crystals of $CeAu_2In_4$ and $LaAu_2In_4$ were grown by a self-flux method using molten In as solvent.[9] High purity chunks of cerium/lanthanum, gold, and indium were loaded into an alumina crucible with a molar ratio of 1:2:20, which was further sealed in an evacuated quartz tube. The loaded quartz tube was heated up to 1050 °C in 12 h and held at that temperature for 48 h to ensure sufficient melting. It was then cooled down to 450 °C in 15 days and dwelled for 2 days. Needle shaped single crystals (length of $\sim$ 5–6 mm) were obtained, after removing excess In by centrifuging at 450 °C. Trace of residual In wetted on the surface of the obtained crystals was removed in dilute hydrochloric acid.

The stoichiometric composition of $CeAu_2In_4$ and $LaAu_2In_4$ crystals was confirmed by energy dispersive x-ray (EDX) spectroscopy using Hitachi S-4800 scanning electron microscope. Considering the existence of two related crystal structures for RAu_2In_4 with light and heavy rare earth atoms, we have also performed single crystal x-ray diffraction studies by employing the Bruker D8 Venture diffractometer, and refined the crystal structure by full-matrix least-squares fitting on the structure factor F^2 using the SHELXL-2014/7 program. Furthermore, the as-grown single crystals were also ground to fine powder and subject to powder x-ray diffraction investigations.

The dc magnetic susceptibility and magnetization measurements were carried out in the magnetic property measurement system (MPMS, Quantum Design). The electrical resistivity was measured from 2 K to room temperature in the physical property measurement system (PPMS, Quantum Design), and also extended down to 0.1 K in a ^{3}He–^{4}He dilution refrigerator, with the electrical current applied along the b-axis, i.e., the needle direction of the single crystal. As complementary to the dc magnetic susceptibility measured down to 2 K, the ac susceptibility was measured between 0.1 K and 2 K in the ^{3}He–^{4}He dilution refrigerator, too, utilizing a lock-in amplifier. The specific-heat measurements were performed by a thermal-relaxation method in the PPMS equipped with a ^{3}He–^{4}He dilution refrigerator insert.

3. Experimeantal results and discussion

Some of the refined crystallographic parameters for $CeAu_2In_4$ based on single crystal x-ray diffraction are summarized in Table 1.

The space group was determined to be *Pnma*, in agreement with the report in Ref. [9]. The powder x-ray diffraction pattern (Fig. 1) of $CeAu_2In_4$ shows good agreement with the calculated one based on the refined crystal structure and

Table 1. Refinement results of the crystal structure and atomic information for $CeAu_2In_4$ obtained at room temperature. U is the equivalent isotropic displacement parameter.

Chemical formula:	$CeAu_2In_4$				
Crystal structure:	Orthorhombic $NdRh_2Sn_4$-type				
Space group:	*Pnma* (No. 62)				
Lattice constants:	$a = 18.4704$ Å, $b = 4.6553$Å, $c = 7.3688$ Å				
Atom	Wyck.	x/a	y/b	z/c	U (eq)
Ce	4c	0.14109(6)	0.25	0.52058(15)	0.0178(4)
Au1	4c	0.53789(4)	0.75	0.75656(11)	0.0192(4)
Au2	4c	0.28212(4)	0.75	0.53142(11)	0.0188(4)
In1	4c	0.68448(8)	0.75	0.6765(2)	0.0174(4)
In2	4c	0.18876(8)	0.75	0.23177(19)	0.0163(4)
In3	4c	0.46518(8)	0.25	0.8534(2)	0.0184(4)
In4	4c	0.43244(9)	0.75	0.4878(2)	0.0204(4)

reveals no secondary phases. The consequently obtained crystal structure is shown in Fig. 2(a) in a view along the *b*-axis. The highlighted shadow part shows the coordination environment of the Ce atom and is further enlarged in Fig. 2(b). The Ce atom is located at the center of a cage, bonding with the surrounding eight In atoms and five Au atoms. Projecting the cages onto the *ab* plane, one sees that Ce atoms form a Ce–Ce chain running along the *b*-axis, surrounded by alternatively stacked Au_2In_3 pentagons and Au_3In_5 octagons (Fig. 2(c)). The nearest Ce–Ce distance is equal to the lattice constant along *b* axis, 4.655 Å. The other two neighboring Ce–Ce distances are about 5.716 Å and 7.368 Å, much larger than the intra chain distance, as reflected by the needle-like morphology (Fig. 2(d)). The Ce–Ce nearest distance (4.655 Å) is considerably large, but being still within the range of varied magnetically ordered Ce-based Kondo compounds, such as $CeIn_3$ (4.69 Å, and $T_N = 10$ K).[14]

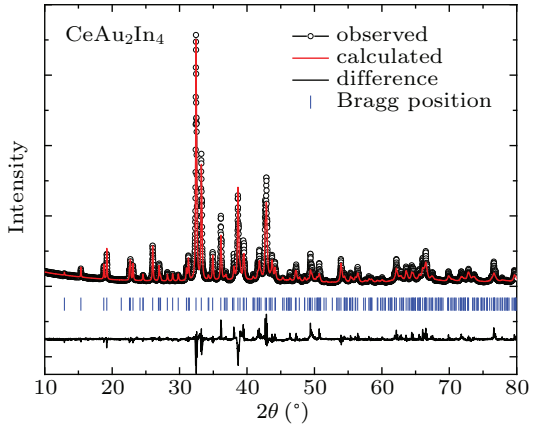


Fig. 1. Powder XRD pattern of $CeAu_2In_4$. The calculated counterpart based on the refined structure (see Table 1) is also shown for comparison.

The dc magnetic susceptibilities measured between 2 K and 300 K with magnetic fields oriented parallel and perpendicular to the *b* axis are shown in Fig. 3(a). A rather strong magnetic anisotropy is observed, with $\chi_{\parallel}/\chi_{\perp} = 6.4$ at $T = 2$ K. No magnetic ordering can be confirmed in this temperature range, in agreement with the report in Ref. [11]. The inverse susceptibility $\chi^{-1}(T)$ (Fig. 3(a) inset) is linear above 100 K following the Curie–Weiss law, with the paramagnetic Curie temperature $\theta_p = 8.57$ K and -42.6 K for $B \parallel b$ and $B \perp b$, respectively, reflecting a strong magnetocrystalline anisotropy. Correspondingly, the effective magnetic moments are estimated to be 2.53 μ_B and 2.59 μ_B, respectively, close to the free moment of trivalent Ce ion, 2.54 μ_B. The ac susceptibility (Fig. 3(b)) measurements performed at lower temperature and in zero bias field in a dilution refrigerator reveal a clear cusp at $T \approx 1.1$ K, characteristic of an antiferromagnetic transition. This temperature is slightly higher than that marked in specific heat ($T_N = 0.9$ K, to be shown below), a situation resembling that in frustrated CePdAl,[15] where frustration-induced short-range spin correlations play a significant role in the vicinity of T_N.

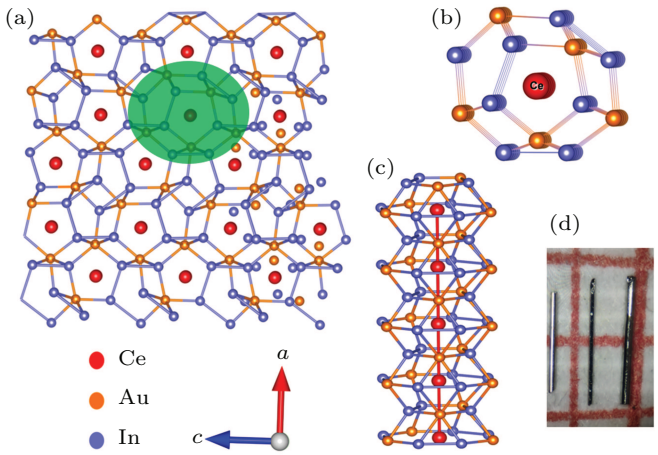


Fig. 2. (a) Crystal structural of $CeAu_2In_4$ viewed along the *b* axis. The shaded part highlights the coordination environment of the Ce atom and is enlarged in panel (b). Panel (c) shows the polyhedral unit extending along the *b* axis, i.e., the needle-like crystal growth direction. Panel (d) displays a photo image of the single crystals employed in this work.

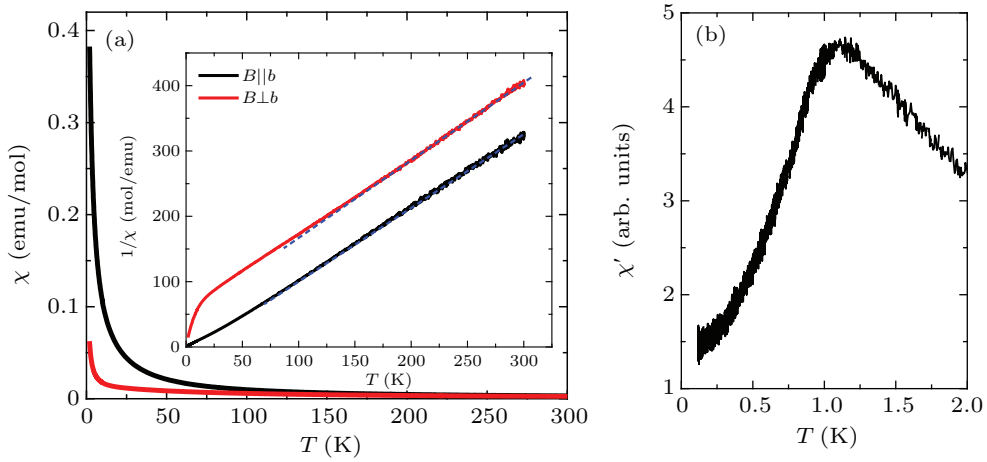


Fig. 3. (a) The dc magnetic susceptibility χ measured in a magnetic field of $B = 0.1$ T applied parallel and perpendicular to the *b* axis. Inset: Inverse susceptibility $1/\chi$ as a function of temperature. (b) The ac susceptibility measured at low temperatures reveals a cusp at 1.1 K, characteristic of an antiferromagnetic phase transition.

Magnetization $M(B)$ measured at $T = 2$ K saturates at 1.9 μ_B for $B \parallel b$, and at 0.5 μ_B for $B \perp b$, see Fig. 4. The saturation moment along b axis is close to the full moment of free Ce^{3+} ion, 2.14 μ_B. Such a large saturation moment is rare in Ce-based heavy-fermion compounds because of the Kondo screening and the crystal-electric-field (CEF) effect. This is, however, not unusual in some cubic Kondo lattices, see, for example, CeSb[16] and CeBi[17] where large saturation moment (2.10 μ_B) has been observed in their respective $M(B)$ curves after the occurrence of a couple of spin-flip transitions. This has been ascribed to the CEF quartet ground state (Γ_8) realized in cubic systems and the low exitation energy of the excited Γ_7 doublet[18] (specifically, the CEF splitting is 37 ± 3 K for CeSb and 8 ± 3 K for CeBi). Given that the lattice is lower-symmetry orthorhombic and the ground state is doublet in $CeAu_2In_4$, as will be confirmed by specific-heat measurements (Fig. 6), the large saturation moment in $CeAu_2In_4$ points to not only a small CEF excitation energy, but also a very weak Kondo effect.

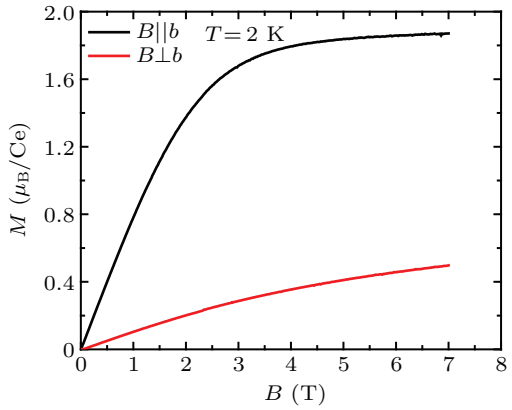


Fig. 4. Magnetization of $CeAu_2In_4$ measured at $T = 2$ K with magnetic field oriented parallel and perpendicular to the b axis.

Figure 5(a) shows the electrical resistivity $\rho(T)$ measured along the b axis for both $CeAu_2In_4$ and $LaAu_2In_4$. Upon cooling from room temperature, $\rho(T)$ of both compounds decrease monotonically, showing rather small absolute resistivity values less than 30 μΩ·cm. Nevertheless, the effect of f electrons in $CeAu_2In_4$ is apparent: $\rho(T)$ of $LaAu_2In_4$ shows weakly negative curvature down to about 30 K and flattens out with further cooling. By contrast, in $\rho(T)$ of $CeAu_2In_4$, the negative curvature extends to an even lower temperature, 10 K, below which an abrupt drop due to AFM transition follows, see Fig. 5(b). The magnetic contribution ρ_{mag}, estimated by subtracting the resistivity of $LaAu_2In_4$ from that of $CeAu_2In_4$, has no clear $-\ln T$ dependence arising from the Kondo scattering, pointing again to a weak Kondo effect of the low-lying CEF multiplet. A rapid decrease of $\rho(T)$ is observed below the AFM transition at $T_N = 0.9$ K, as is marked by a peak in the derivative of $\rho(T)$, see inset of Fig. 5(b). This is the same temperature at which magnetic order is detected in specific heat, see Fig. 6(a). At $T < T_N$, $\rho(T)$ can be described by the Fermi liquid description, $\rho = \rho_0 + AT^2$, with $A = 0.20$ μΩ·cm·K^{-2}, see the dashed line in Fig. 5(b).

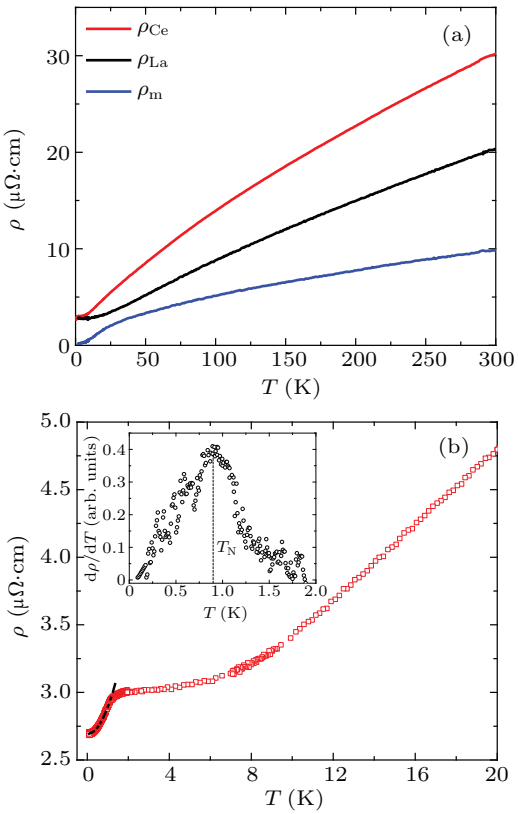


Fig. 5. (a) Resistivity $\rho(T)$ of both $CeAu_2In_4$ and $LaAu_2In_4$, as well as the magnetic contribution $\rho_m(T)$ to the former estimated as being their difference. (b) The low-temperature part of $\rho(T)$ for $CeAu_2In_4$. The dashed line is a fitting to the Fermi liquid description $\rho = \rho_0 + AT^2$ at $T < T_N$, with $A = 0.20$ μΩ·cm·K^{-2}. Inset shows the low temperature variation of the temperature derivative of the resistivity, where the maximum marks the position of the AFM transition at $T_N = 0.9$ K.

Figure 6(a) shows the low-temperature specific heat $C(T)$ of $CeAu_2In_4$ and $LaAu_2In_4$, and the magnetic contribution $C_m(T)$ to the former that is estimated as the difference between them. A marked peak at $T = 0.9$ K confirms the onset of the AFM transition. At $T > T_N$, $C_m(T)$ increases upon cooling from 5 K, a temperature more than five times higher than T_N. Consequently, the specific-heat peak due to the AFM ordering is rather symmetric, deviating largely from a typical mean-field-like second order phase transition. Such a symmetric broadening of the AFM transition in specific heat is probably attributable to the spin fluctuations favored by one dimensionality. It is reminiscent of specific heat peak profile recently observed in CePdAl,[19] a spin-frustrated Kondo lattice with a strongly reduced value of T_N. The magnetic entropy S_m is estimated by integrating the values of $C_m(T)/T$ with respect to T and shown in Fig. 6(b). The magnetic entropy $S_m(T)$ released below T_N, 3.5 J/mol·K, is much smaller than $R\ln 2 = 5.76$ J·mol^{-1}·K^{-1}, the entropy associated with the Kramers doublet ground state. The full entropy of the magnetic doublet ground state is recovered at 2.5 K, a tem-

perature more than double of the magnetic transition temperature, and remains flat until at least 5 K. These indicate that the magnetic order arises from the low-lying Kramers doublet of the CEF state of the Ce^{3+} multiplets. The reduced entropy at T_N can be approached from two alternative scenarios: One is the Kondo effect and the other the enhanced spin fluctuations related to low dimensionality. According to Desgranges and Schotte's calculation of specific heat and magnetic entropy using the Bethe ansatz for a spin-1/2 Kondo model,[20] the magnetic entropy released at the characteristic temperature T_N is related to the ratio T_N/T_K. The calculated entropy of $0.61R\ln 2 = 3.5$ J/(mol·K) at T_N in $CeAu_2In_4$ yields $T_N/T_K = 0.8$ and therefore $T_K = 1.1$ K. The obtained value of T_K is very close to T_N, indicating a comparable competition between the RKKY interaction and the Kondo effect in $CeAu_2In_4$. Note that, this estimation assumes that the magnetic entropy reduction is fully caused by the Kondo effect and ignores the spin fluctuations resulting from low dimensionality, and therefore will overestimate the value of T_K.[21]

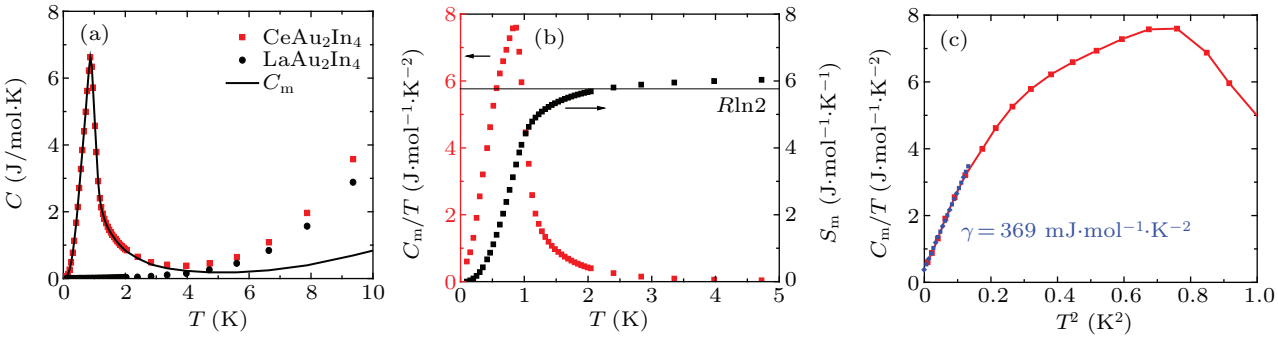


Fig. 6. (a) Low-temperatures specific heat of $CeAu_2In_4$ and $LaAu_2In_4$. Note the non-mean-field-like peak at T_N, which arises from the strong quantum fluctuations developed far above T_N. (b) Magnetic specific heat shown as C_m/T vs. T (left) and the corresponding magnetic entropy $S_m(T)$ estimated by integrating C_m/T with respect to T. (c) $C(T)/T$ vs. T^2 for $T < 1$ K, from which the Sommerfeld coefficient can be estimated as $\gamma = 369$ mJ·mol^{-1}·K^{-2} by extrapolating the linear part to zero temperature.

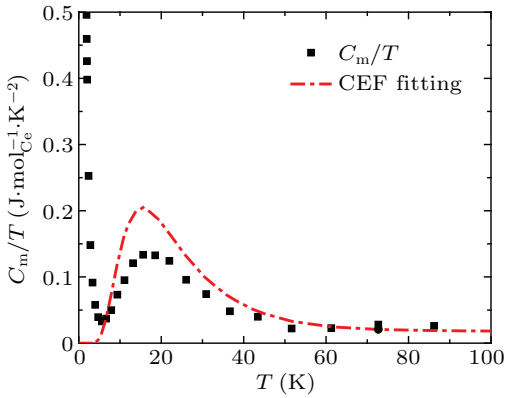


Fig. 7. Magnetic contribution to the specific heat, C_m/T, as a function of temperature. A Schottky maximum due to CEF splitting of the Ce^{3+} multiplets appears at about 15.8 K. The dashed red line calculated simply from three-doublet CEF scheme with $E_1 = 50$ K and $E_2 = 400$ K is shown and can describe the Schottky anomaly reasonably well.

Given such a small T_K and the weak CEF splitting which assumes large Schottky anomaly extending down to low temperatures, one cannot rely on $C(T)$ above T_N to estimate the Sommerfeld value of γ. Focusing on the temperature window well below T_N, where the Fermi-liquid behavior has been observed in resistivity (Fig. 5(b)), we estimated the Sommerfeld coefficient to be $\gamma = 369$ mJ·mol^{-1}·K^{-2} by extrapolating the linear function of $C(T)/T$ vs. T^2 below 0.4 K down to zero temperature, see Fig. 6(c). A large γ value within the ordered phase indicates strong spin fluctuations in the ground state. The consequently obtained KW ratio, $A/\gamma^2 = 1.47 \times 10^{-6}$ μΩ·cm (K·mol/mJ)^2, is one order of magnitude smaller than that of common heavy fermion materials, 10^{-5} μΩ·cm (K·mol/mJ)^2.[22] The latter value applies to heavy-fermion materials with doublet ground state, when the CEF splitting energy $E_i > T_K$.[23] Presumably, the reduced KW ratio observed in $CeAu_2In_4$ arises from the ground state spin fluctuations induced by low dimensionality, which contribute directly to the low-temperature specific heat, but is less influential to electrical resistivity.

To shed light on the reduced KW ratio and also to elucidate the large saturation moment, here we look into the high-temperature $C_m(T)$ and evaluate the CEF scheme acting on the Ce ions. It is known that the $J = 5/2$ ground state in the orthorhombic lattice of $CeAu_2In_4$ is split into three doublets,[11] and the first and second excited energy levels were estimated to be $E_1 = 73$ K and $E_2 = 412$ K based on magnetic susceptibility measurements. Our experimental results of C_m/T vs. T (Fig. 7) exhibits a Schottky peak at $T = 15.8$ K. The red line of Fig. 7 is the best fitting based on the three-doublet scheme, with a Kramers doublet ground state and two excited doublets at $E_1 = 50$ K and $E_2 = 400$ K. The small CEF splitting can be partly explained by the cage-like structure of $CeAu_2In_4$, in which the surrounding Au–In polyhedral have an effect of isolating the rare earth ions from each other. Considering the relatively small CEF splitting, it is tempted to ascribe the reduced KW ratio to a quasi-quartet CEF ground state, where such behavior has been rationalized theoretically.[23] However, this explanation seems unlikely for $CeAu_2In_4$ because its Kondo temperature T_K is far smaller than the CEF splitting energies

and the heavy-fermion liquid phase is born completely from the many-body state of the low-lying Kramers doublet.

Surprisingly, similar KW ratio (A/γ^2) as observed in $CeAu_2In_4$ has also been found in the prototypical q1D Kondo-lattice compound $YbNi_4P_2$ (Ref. [13]) and $CeRh_6Ge_4$ (Ref. [7]). The latter two compounds are located in the vicinity of a FM QCP. Likewise, both $YbNi_4P_2$ and $CeRh_6Ge_4$ exhibit a considerably low magnetic ordering temperature, subject to strong quantum fluctuations. Specifically, $YbNi_4P_2$ orders ferromagnetically at $T_C = 0.17$ K and has a Kramers doublet ground state separated from the first excited energy level by $E_1 = 8.5$ meV.[24] $CeRh_6Ge_4$ shows a FM transition at $T_C = 2.5$ K[25] associated with a Kramers doublet ground state, too. The excited CEF doublets for $CeRh_6Ge_4$ were verified by Shu *et al.* at $E_1 = 5.8$ meV and $E_2 = 22.1$ meV.[26] The Kondo temperatures for these two compounds are relatively small, being $T_K = 8$ K for $YbNi_4P_2$ and $T_K = 19$ K for $CeRh_6Ge_4$. Given the q1D nature and the strong quantum fluctuations in proximity to magnetic ordering in all these compounds, it is natural to speculate a common origin underlying the unusual KW ratio. Namely, the low-dimensionality induced spin fluctuations bring about the unusually enhanced value of γ and hence the reduced KW ratio in all these q1D Kondo compounds.

4. Summary

To summarize, we have synthesized single crystals of $CeAu_2In_4$ and its nonmagnetic reference compound $LaAu_2In_4$ by self-flux method, both of which form needle-like morphology. Single crystal x-ray diffraction analysis indicates that $CeAu_2In_4$ adopts an orthorhombic structure with the nearest Ce–Ce distance along the needle direction. Combined electrical resistivity, ac and dc magnetic susceptibilities, and specific-heat measurements at low temperatures verify an antiferromagnetic transition at $T_N = 0.9$ K. Magnetic contribution to the electrical resistivity reveals no apparent $-\ln T$ dependence, suggestive of a very weak Kondo effect. However, the electronic specific-heat coefficient $\gamma = 369$ mJ/mol·K^2 at zero temperature limit is large, and the magnetic entropy released below T_N is strongly reduced from $R\ln 2$. We argue that the low-dimensionality-induced spin fluctuations rather than the weak Kondo effect play a significant role in determining the thermodynamics of the ground-state doublet. In line with this argument, we found that the Kadowaki–Woods ratio A/γ^2 for $CeAu_2In_4$ is nearly a factor-of-ten smaller than that expected for heavy-fermion materials with Kramers doublet ground state, a feature that shares striking similarity to other q1D Kondo-lattice compounds like $YbNi_4P_2$ and $CeRh_6Ge_4$. The low-dimensionality-induced spin fluctuations are believed to be underlying the unusual KW ratio observed in all these q1D Kondo compounds. Further investigations along this line appear to be highly interesting in view of the potential novel quantum critical behaviors associated with the enhanced spin fluctuations. At last, we note that the isomorphic RAu_2In_4 also forms for light rare earth Pr and Nd (Ref. [9]), and both compounds are non-magnetic above 2 K resembling $CeAu_2In_4$, calling for further investigations as well.

References

[1] Shimozawa M, Goh S K, Shibauchi T and Matsuda Y 2016 *Rep. Prog. Phys.* **79** 074503
[2] Shishido H, Shibauchi T, Yasu K, Kato T, Kontani H, Terashima T and Matsuda Y 2010 *Science* **327** 980
[3] Doniach S 1977 *Physica B+C* **91** 231
[4] Custers J, Gegenwart P, Wilhelm H, Neumaier K, Tokiwa Y, Trovarelli O, Geibel C, Steglich F, Pépin C and Coleman P 2003 *Nature* **424** 524
[5] Izawa K, Yamaguchi H, Matsuda Y, Shishido H, Settai R and Onuki Y 2001 *Phys. Rev. Lett.* **87** 057002
[6] Steppke A, Kuchler R, Lausberg S, Lengyel E, Steinke L, Borth R, Luhmann T, Krellner C, Nicklas, Geibel M C, Steglich F and Brando M 2013 *Science* **339** 933
[7] Shen B, Zhang Y, Komijani Y, Nicklas M, Borth R, Wang A, Chen Y, Nie Z, Li R, Lu X, Lee H, Smidman M, Steglich F, Coleman P and Yuan H 2020 *Nature* **579** 51
[8] Wang L, Fu Z, Sun J, Liu M, Yi W, Yi C, Luo Y, Dai Y, Liu G, Matsushita Y, Yamaura K, Lu L, Cheng J G, Yang Y F, Shi Y and Luo J 2017 *npj Quantum Materials* **2** 36
[9] Salvador J R, Hoang K, Mahanti S D and Kanatzidis M G 2007 *Inorg. Chem.* **46** 6933
[10] Sebastian C P, Salvador J, Martin J B and Kanatzidis M G 2010 *Inorg. Chem.* **49** 10468
[11] Joshi D A, Manfrinetti P, Dhar S K and Thamizhavel A 2010 *J. Phys.: Conf. Ser.* **200** 012074
[12] Paschen S and Si Q 2020 *Nat. Rev. Phys.* **3** 9
[13] Pfau H, Daou R, Friedemann S, Karbassi S, Ghannadzadeh S, Küchler R, Hamann S, Steppke A, Sun D, König M, Mackenzie A P, Kliemt K, Krellner C and Brando M 2017 *Phys. Rev. Lett.* **119** 126402
[14] Buschow K H J, de Wijn H W and van Diepen A M 1969 *J. Chem. Phys.* **50** 137
[15] Zhao H, Zhang J, Hu S, Isikawa Y, Luo J, Steglich F and Sun P 2016 *Phys. Rev. B* **94** 235131
[16] Busch G and Vogt O 1967 *Phys. Lett. A* **25** 449
[17] Bartholin H, Florence D, Wang T and Vogt O 1974 *Phys. Stat. Sol.* **24** 631
[18] Heer H, Furrert A, Halgt W and Vogt O 1979 *J. Phys. C: Solid State Phys.* **12** 5207
[19] Fritsch V, Huang C L, Bagrets N, Grube K, Schumann S and Löhneysen H v 2013 *Physica Status Solidi (b)* **250** 506
[20] Desgranges H U and Schotte K D 1982 *Phys. Lett. A* **91** 240
[21] Yashima H 1982 *Solid State Commun.* **43** 193
[22] Kadowaki K and Woods S 1986 *Solid State Commun.* **58** 507
[23] Tsujii N, Kontani H and Yoshimura K 2005 *Phys. Rev. Lett.* **94** 057201
[24] Huesges Z, Kliemt K, Krellner C, Sarkar R, Klauß H H, Geibel C, Rotter M, Novák P, Kuneš J and Stockert O 2018 *New J. Phys.* **20** 073021
[25] Voßwinkel D, Niehaus O, Rodewald U C and Pöttgen R 2012 *Zeitschrift für Naturforschung B* **67** 1241
[26] Shu J W, Adroja D T, Hillier A D, Zhang Y J, Chen Y X, Shen B, Orlandi F, Walker H C, Liu Y, Cao C, Steglich F, Yuan H Q and Smidman M 2021 arXiv:2102.12788